Supplement of Geosci. Model Dev., 14, 907–921, 2021
https://doi.org/10.5194/gmd-14-907-2021-supplement

Geoscientific Model Development
Open Access
EGU

Supplement of

A zero-dimensional view of atmospheric degradation of levoglucosan (LEVCHEM_v1) using numerical chamber simulations

Loredana G. Suciu et al.

Correspondence to: Loredana G. Suciu (lgs4@rice.edu)

S1 Levoglucosan and the products of its chemical degradation

The chemical structure of levoglucosan (LEV) and its gas-phase and aerosol-phase degradation products (LEVP#) are shown in Figure S1. Products LEVP1, LEVP2, LEVP3 and LEVP5 are generated in both phases (gas and aerosol), product LEVP4 is generated only in the gas phase, and products LEVP6 and LEVP7 are generated only in the aerosol phase. However, because the last three products can partition between phases via either evaporation or condensation, they are also considered degradation products in both the aerosol and gas phase. Henceforth, in their respective chemical mechanism, they are labeled as LEVP#_G or LEVP#_A, in which letters G and A refer to gas-phase and aerosol-phase, respectively. The chemical structures of LEV and LEVP1-LEVP4 are adapted from Bai et al. (2013) and those of LEVP6-LEVP7 are modeled with Chem3D 16.0, following the structures from Kessler et al. (2010). The chemical structure of LEVP5, also created with Chem3D 16.0, is introduced here for the first time based on the similarity of the reaction between an organic compound and N_2O_5 described by Gross et al. (2009). Intermediary or radical products are shown in Figure S2. The chemical structures of LEVR, LEVRO, LEVRO2 and LEVROOH are adapted from Bai et al. (2013), while that of LEVR1 is re-created using Chem3D 16.0, based on Kessler et al. (2010). Radicals are also common to both phases as they are generated by the phase-specific chemical mechanisms, but they are not considered in the G/P mechanism based on the assumption that they react very quickly once produced.

LEV

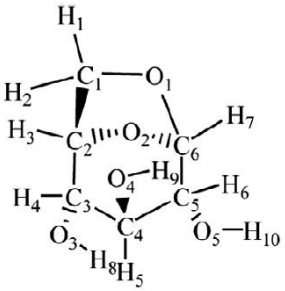

LEVP2

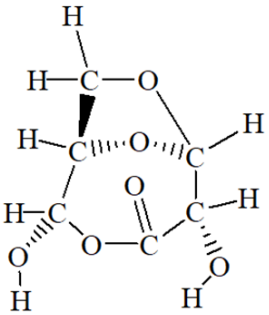

LEVP4

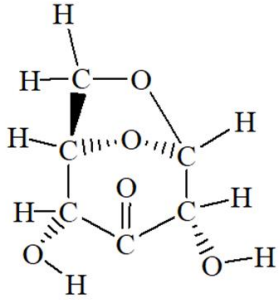

LEVP6

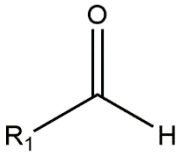

LEVP1

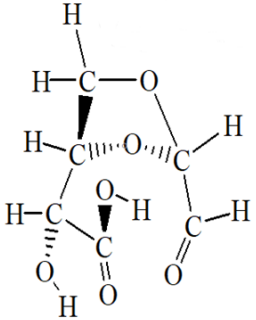

LEVP3

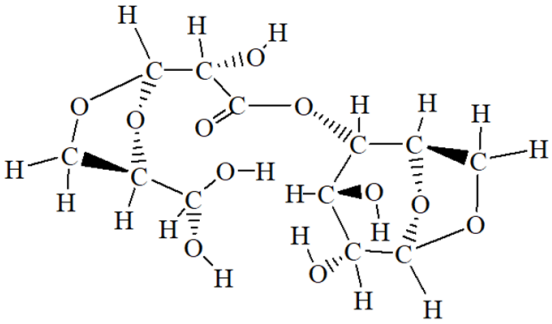

LEVP5

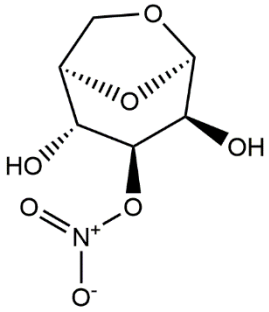

LEVP7

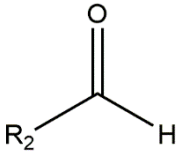

Figure S1: Chemical structures of levoglucosan and its degradation products

LEVR

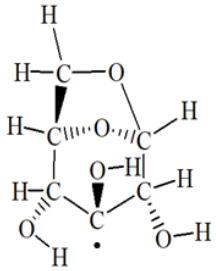

LEVR1

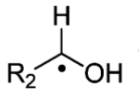

LEVRO

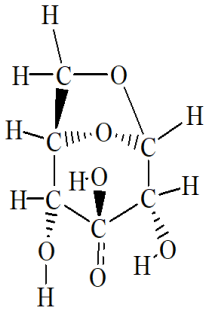

LEVRO2

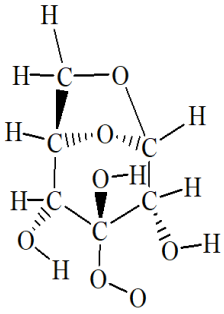

LEVROOH

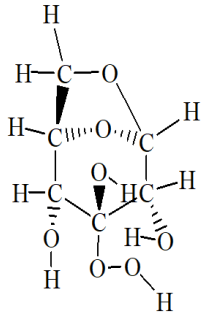

Figure S2: Chemical structures of intermediary (radical) products of levoglucosan degradation

S2 Main conditions and parameters used in chamber simulations

The initial conditions of LEV concentration in both phases and main parameters used in the chamber simulations are given in Table S1. Note that the BOXMOXv1.7 model used to develop LEVCHEM_v1 does not explicitly model relative humidity, but it does model H_2O vapor concentration. Therefore, the values of RH used in chamber experiments were converted to H_2O vapor concentration and used in the simulations to roughly reproduce the conditions used in chamber experiments from the three studies (Hennigan et al., 2010; Lai et al., 2014; Pratap et al., 2019). All simulations were conducted at ambient atmospheric pressure (1013.35 hPa). Total aerosol number concentration (N_t) and surface area density (SAD) were taken or calculated based on Seinfeld and Pandis (2006). Enthalpy of vaporization ($\Delta H_{vap,i}$) at 298.15 K was taken from Xie et al. (2014) and applied to all species (both LEV and its products) that were subjected to the gas-particle (G/P) partitioning mechanism. Surface tension (σ) of LEV and related species was assumed to be similar to that of benzene and taken from Seinfeld and Pandis (2006). Saturation concentration of organics at 298 K ($C_i^*(298\ K)$) was taken from May et al. (2012). The bulk density of the particle (ρ) was assumed to be the density of LEV. The diffusion coefficient for organic vapors in air (D) was taken from May et al. (2013) and assumed to be the same for all LEV-related species.

Table S1 Conditions used in chamber simulations for model evaluation

Reference study	LEV_G_0 (ppmv)*	LEV_A_0 (ppmv)	H_2O (ppmv)	RH (%)	T (K)	D_p (m)	N_t (m^{-3})	SAD (m^{-1})	$\Delta H_{vap,i}$ (J mol^{-1})	σ (N m^{-1})	$C_i^*(298\ K)$ (kg m^{-3})	ρ (kg m^{-3})	D (m^2 s^{-1})
Hennigan et al. (2010)	$9.62x10^{-2}$	$6.23x10^{-3}$	$2.22x\ 10^{3}$	10	293.15	$5x10^{-7}$	$3.18x10^{7}$	$2.50x10^{-5}$	$84x10^{3}$	$2.82x10^{-2}$	$13x10^{-9}$	$1.69x10^{3}$	$5x10^{-6}$
Lai et al. (2014)	$9.62x10^{-2}$	$7.09x10^{-4}$	$1.18x10^{4}$	40	298.15	$2x10^{-7}$	$9.96x10^{8}$	$1.25x10^{-4}$	$84x10^{3}$	$2.82x10^{-2}$	$13x10^{-9}$	$1.69x10^{3}$	$5x10^{-6}$
	$9.62x10^{-2}$	$7.09x10^{-4}$	$6.60x10^{3}$	40	288.15	$2x10^{-7}$	$9.96x10^{8}$	$1.25x10^{-4}$	$84x10^{3}$	$2.82x10^{-2}$	$13x10^{-9}$	$1.69x10^{3}$	$5x10^{-6}$
Pratap et al. (2019)	$9.62x10^{-2}$	$7.23x10^{-3}$	$3.63x10^{3}$	30	283.15	$2x10^{-7}$	$9.96x10^{8}$	$1.25x10^{-4}$	$84x10^{3}$	$2.82x10^{-2}$	$13x10^{-9}$	$1.69x10^{3}$	$5x10^{-6}$

*The initial gas-phase LEV concentration was determined from its vapor pressure.

S3 Evolution of LEV degradation products and their relative importance

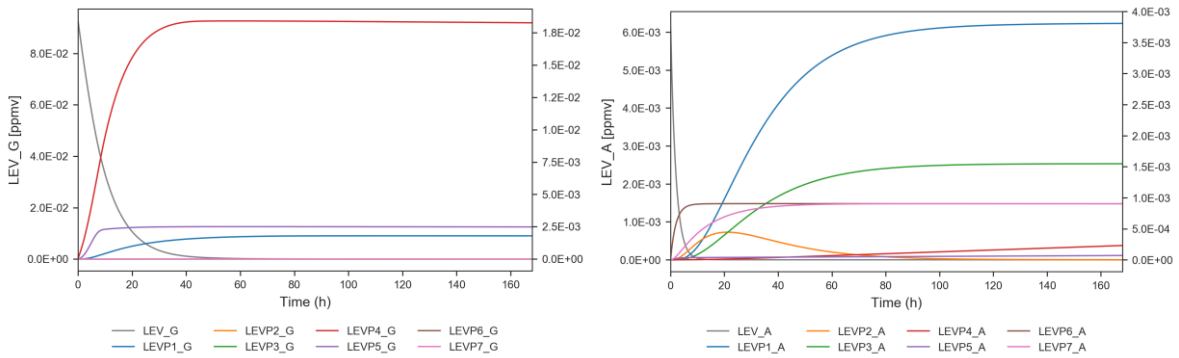

Figure S3: Products of LEV degradation in the gas phase (left) and the aerosol phase (right). (F = 0.02; α = 0.1) (simulated conditions based on Hennigan et al. (2010)). Concentration of products (ppmv) is displayed on the secondary y-axis.

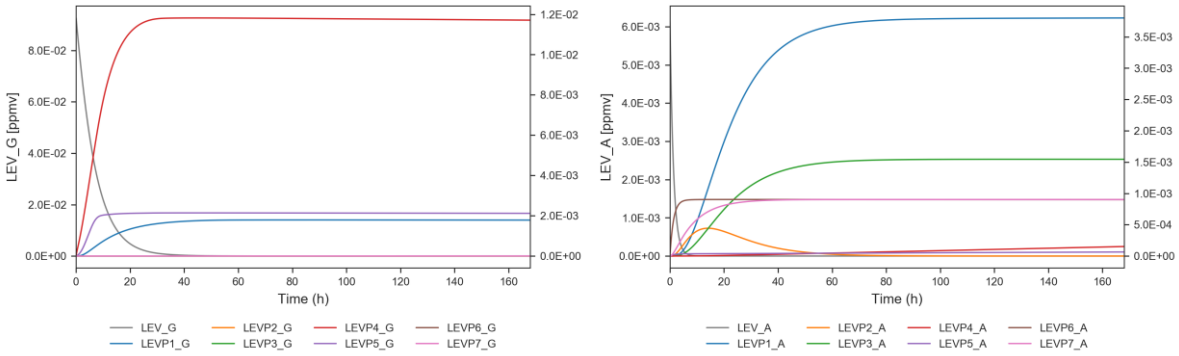

Figure S4: Products of LEV degradation in the gas phase (left) and the aerosol phase (right). (F = 0.03; α = 0.1) (simulated conditions based on Hennigan et al. (2010)). Concentration of products (ppmv) is displayed on the secondary y-axis.

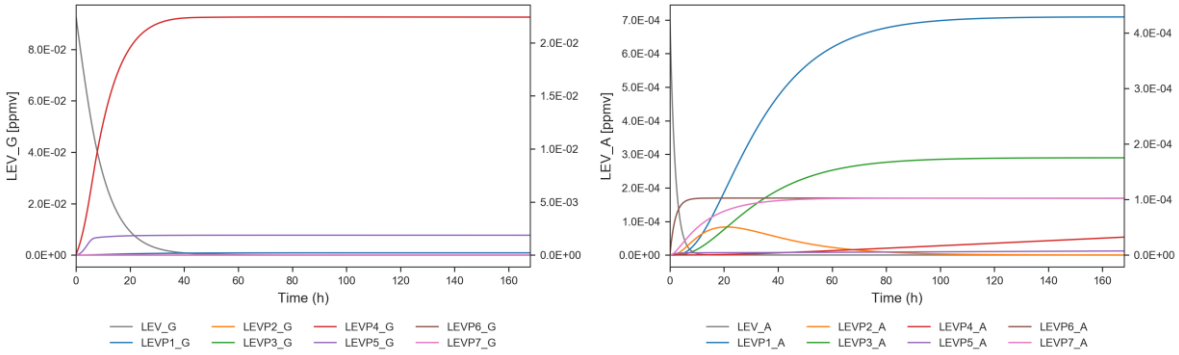

Figure S5: Products of LEV degradation in the gas phase (left) and the aerosol phase (right). (F = 0.004; α = 0.01) (simulated conditions based on Lai et al. (2014)). Concentration of products (ppmv) is displayed on the secondary y-axis.

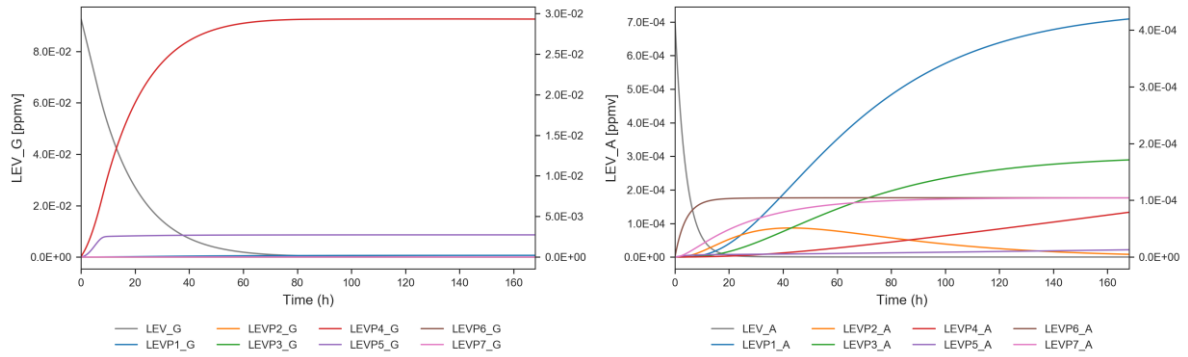

Figure S6: Products of LEV degradation in the gas phase (left) and the aerosol phase (right). (F = 0.002; α = 0.01) (simulated conditions based on Lai et al. (2014)). Concentration of products (ppmv) is displayed on the secondary y-axis.

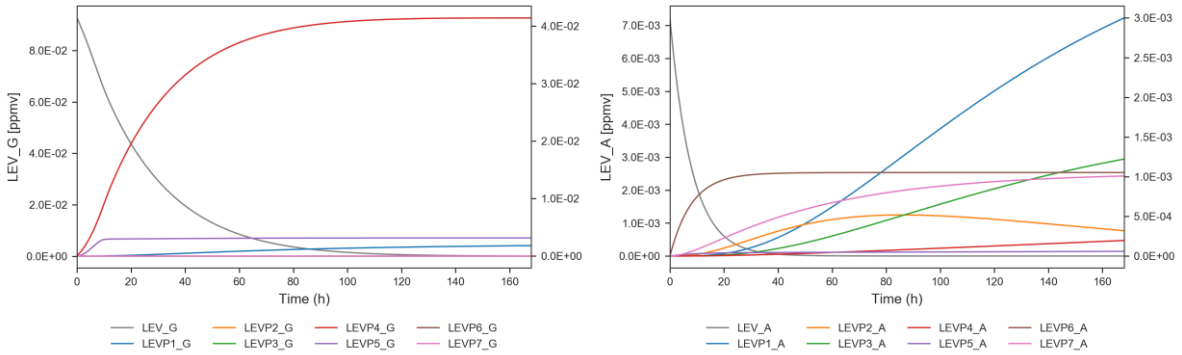

Figure S7: Products of LEV degradation in the gas phase (left) and the aerosol phase (right). (F = 0.001; α = 0.01) (simulated conditions based on Pratap et al. (2019)). Concentration of products (ppmv) is displayed on the secondary y-axis.

References

Bai, J., Sun, X., Zhang, C., Xu, Y.and Qi, C.: The OH-initiated atmospheric reaction mechanism and kinetics for levoglucosan emitted in biomass burning, Chemosphere, 93, 2004–2010, https://doi.org/10.1016/j.chemosphere.2013.07.021, 2013.

Gross, S., Ianonne, R., Xiao, S. and Bertram, A. K.: Reactive uptake studies of NO3 and N2O5 on alkenoic acid, alkanoate, and polyalcohol substrates to probe nighttime aerosol chemistry, Phys. Chem. Chem. Phys., 11, 7792-7803, https://doi.org/10.1039/B904741G, 2009.

Hennigan, C.J., Sullivan, A. P., Collett, J. L. and Robinson, A. L.: Levoglucosan stability in biomass burning particles exposed to hydroxyl radicals, Geophys. Res. Lett., 37, https://doi.org/10.1029/2010GL043088, 2010.

Kessler, S. H., Smith, J. D., Che, D. L., Worsnop, D. R., Wilson, K. R. and Kroll, J. H.: Chemical sinks of organic aerosol: kinetics and products of the heterogeneous oxidation of erythritol and levoglucosan, Environ. Sci. Technol., 44, 7005–7010, https://doi.org/10.1021/es101465m, 2010.

Lai, C., Liu, Y., Ma, J., Ma, Q. and He, H.: Degradation kinetics of levoglucosan initiated by hydroxyl radical under different environmental conditions, Atmos. Environ., 91, 32–39, https://doi.org/10.1016/j.atmosenv.2014.03.054, 2014.

May, A. A., Saleh, R., Hennigan, C. J., Donahue, N. M. and Robinson, A. L.: Volatility of organic molecular markers used for source apportionment analysis: measurements and implications for atmospheric lifetime, Environ. Sci. Technol., 46, 22, 12435-12444, https://doi.org/10.1021/es302276t, 2012.

Pratap, V., Bian, Q., Kiran, S. A., Hopke, P. K., Pierce, J. R. and Nakao, S.: Investigation of levoglucosan decay in wood smoke smog-chamber experiments: The importance of aerosol loading, temperature, and vapor wall losses in interpreting results, Atmos. Environ., 199, 224–232, https://doi.org/10.1016/j.atmosenv.2018.11.020, 2019.

May, A. A., Levin, E. J. T., Hennigan, C. J., Riipinen, I., Lee, T., Collett, J. L., Jimenez, J. L., Kreidenweis, S. M. and Robinson, A. L.: Gas-particle partitioning of primary organic aerosol emissions: 3. Biomass burning, J. Geophys. Res.- Atmos., 118, 11,327–11,338, https://doi.org/10.1002/jgrd.50828, 2013.

Seinfeld, J. H. and Pandis, S. N.: Atmospheric chemistry and physics: from air pollution to climate change, John Wiley & Sons, Inc, Hoboken, NJ, 2006.

Xie, M., Hannigan, M. P. and Barsanti, K. C.: Gas/particle partitioning of 2-methyltetrols and levoglucosan at an urban site in Denver, Environ. Sci. Technol., 48, 2835–2842, https://doi.org/10.1021/es405356n, 2014.